A Letters Journal Exploring the Frontiers of Physics

April 2010

EPL, **90** (2010) 27007
doi: 10.1209/0295-5075/90/27007

www.epljournal.org

Finite-temperature atomic structure of 180° ferroelectric domain walls in $PbTiO_3$

A. Angoshtari and A. Yavari[(a)]

School of Civil and Environmental Engineering, Georgia Institute of Technology - Atlanta, GA 30332, USA

received 24 December 2009; accepted in final form 15 April 2010
published online 19 May 2010

PACS 75.60.Ch – Domain walls and domain structure
PACS 77.80.Dj – Domain structure; hysteresis

Abstract – In this letter we obtain the finite-temperature structure of 180° domain walls in $PbTiO_3$ using a quasi-harmonic–lattice dynamics approach. We obtain the temperature dependence of the atomic structure of domain walls from 0 K up to room temperature. We also show that both Pb-centered and Ti-centered 180° domain walls are thicker at room temperature; domain wall thickness at $T = 300$ K is about three times larger than that of $T = 0$ K. Our calculations show that Ti-centered domain walls have a lower free energy than Pb-centered domain walls and hence are more likely to be seen at finite temperatures.

Introduction. – Ferroelectric perovskites have been the focus of intense research in recent years because of their potential applications in high-strain actuators, high-density storage devices, etc. [1]. It is known that macroscopic properties of ferroelectrics strongly depend on domain walls, which are extended two-dimensional defects. Any fundamental understanding of ferroelectricity in perovskites requires a detailed understanding of domain walls in the nanoscale (see [2] and references therein). Theoretical studies of domain walls have revealed many of their interesting features. From both theoretical calculations and experimental works, it has been observed that the thickness of domain walls can vary from thin walls, which consist of only a few atomic spaces to thick walls, which are in the order of a few micrometers. There have been studies using *ab inito* calculations [3–5] and anaharmonic-lattice statics calculations [6] suggesting that ferroelectric domain walls are atomically sharp. Hlinka and Marton [7] analyzed 90° domain walls in $BaTiO_3$-like crystals in the framework of the phenomenological Ginzburg-Landau-Devonshire (GLD) model and obtained a domain wall thickness of 3.6 nm at room temperature. Chrosch and Salje [8] measured the domain wall thickness in $LaAlO_3$ in the temperature range 295–900 K by X-ray diffraction. They observed that the domain wall thickness increases from about 20 Å to 200 Å and that the variation of domain wall thickness with temperature is linear at low temperatures. Using scanning probe microscopy, Iwata *et al.* [9] found complex 180° domain walls with thicknesses 1–2 μm in PZN-20% PT. Lehnen *et al.* [10] investigated 180° domain walls in $PbTiO_3$ using electrostatic force microscopy (EFM) and piezoelectric force microscopy (PFM) and observed thick 180° domain walls at room temperature with thickness of about 5 μm. Shilo *et al.* [11] studied the structure of 90° domain walls in $PbTiO_3$ by measuring the surface profile close to emerging domain walls and then fitting it to the soliton-type solution of GLD theory. Using this technique they observed that the domain wall thickness is about 1.5 nm but with a wide scatter. They suggested that the presence of point defects within the domain wall is responsible for such variations. Lee *et al.* [12] provided a model to investigate the effect of point defects on the domain wall thickness. See also [13] for a similar study.

Domain walls have been studied using different techniques in the atomic scale at $T = 0$ K. However, one would be interested to know how different the structure and thickness of a 180° domain wall at room temperature are compared to those at $T = 0$ K. In this letter, we study the structure of Pb- and Ti-centered 180° domain walls in $PbTiO_3$ as a function of temperature in some detail. We first start with the static configuration of domain walls and iteratively optimize the free energy for a small temperature, *e.g.* $T_1 = 5$ K. The optimized structure at T_1 will be the reference configuration for a higher temperature $T_2 = T_1 + \Delta T$. Continuing in this way we optimize the structure of the domain wall up to $T = 300$ K. This temperature range is where quantum effects are

[(a)] E-mail: arash.yavari@ce.gatech.edu

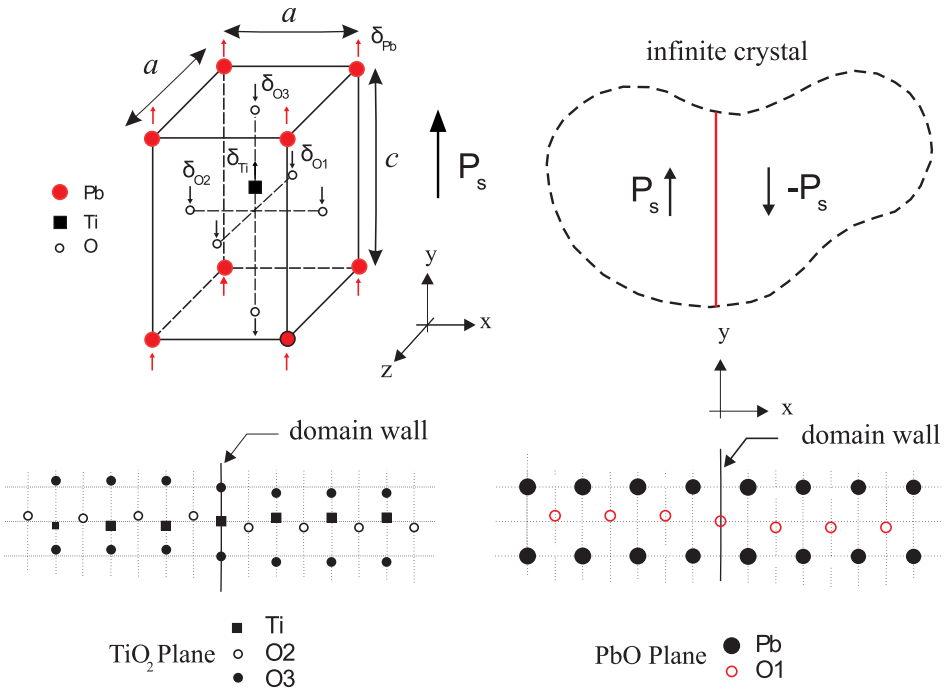

Fig. 1: (Colour on-line) Reference configuration of a Ti-centered 180° domain wall shown in both the TiO_2 and PbO planes. Note that cores and shells on the domain wall have no relative shifts and cores and shells on the left and right sides of the wall have opposite relative shifts.

important and hence molecular-dynamics simulations cannot be used. This is also the temperature range where a quasi-harmonic approximation is reasonable.

Method of calculation. – The geometry of a Ti-centered 180° domain wall is shown in fig. 1. The domain wall is in a (100)-plane and the polarization vector is in the y-direction and changes by 180° across the domain wall. In this geometry, depending on which cations are placed on the domain wall, two types of domain walls are possible: Pb-centered and Ti-centered. In this work, we consider both types and calculate their finite-temperature structures. For our calculations, we use the shell potential developed by Asthagiri *et al.* [14] for $PbTiO_3$. In this potential, each ion is described by a core and a massless shell. The short-range interactions between Pb-O, Ti-O and O-O shells are described by the Rydberg potential $V_{sr}(r) = (A + Br)\exp(-r/C)$, where A, B and C are potential parameters. The cores and shells of each ion have Coulombic interactions with cores and shells of all the other ions. The core and shell of an atom interact by an anharmonic spring of the form $V_{cs}(r) = (1/2)k_2 r^2 + (1/24)k_4 r^4$, where k_2 and k_4 are constants.

The structure of a domain wall is calculated by an analytical free-energy optimization method. This method was developed by Kantorovich [15] and has been applied to various different systems, *e.g.* in [16–18]. We refer the reader to these references for the complete details of the method. A domain wall is an example of a defective lattice with a 1D symmetry reduction [19,20]. Here we briefly explain the free-energy optimization method exploiting symmetry reduction. For more details see [21].

The multi-lattice of $PbTiO_3$ can be partitioned into the union of some 2D equivalence classes that are parallel to the domain wall. Therefore, we reduce the dimension of the problem from three to one, *i.e.*, we can write $\mathcal{L} = \bigsqcup_I \bigsqcup_{\alpha\in\mathbb{Z}} \mathcal{L}_{I\alpha}$, where $\mathcal{L}$, $\mathcal{L}_{I\alpha}$, and $\mathbb{Z}$ are the lattice, 2D equivalence classes, and the set of integers, respectively. Note that $j = J\beta$ means that the atom j is in the β-th equivalence class of the J-th sublattice [19]. As an approximation similar to that of [22], we assume only a finite number of neighboring equivalence classes, N, on each side of the domain wall and assume a temperature-dependent bulk configuration outside this region. Therefore, the size of the effective dynamical matrix would be $15 \times 2N$. To obtain the lattice structure around the domain wall at a finite temperature, we minimize the Helmholtz free energy $\mathcal{F}$, calculated based on the quasi-harmonic approximation with respect to the configuration $\{\mathbf{X}^j\}_{j\in\mathcal{L}}$ at a finite temperature T. Note that away from the domain wall the two half-lattices approach their temperature-dependent configurations. We can write the free energy of the defective lattice $\mathcal{F} \equiv \mathcal{F}\left(\{\mathbf{X}^j\}_{j\in\mathcal{L}}, T\right)$, as

$$\mathcal{F} = \mathcal{E}\left(\{\mathbf{X}^j\}_{j\in\mathcal{L}}\right) + \sum_{\mathbf{k}}\sum_{i}\left\{\frac{1}{2}\hbar\omega_i(\mathbf{k}) + k_B T \ln\left[1 - \exp\left(-\frac{\hbar\omega_i(\mathbf{k})}{k_B T}\right)\right]\right\}, \tag{1}$$

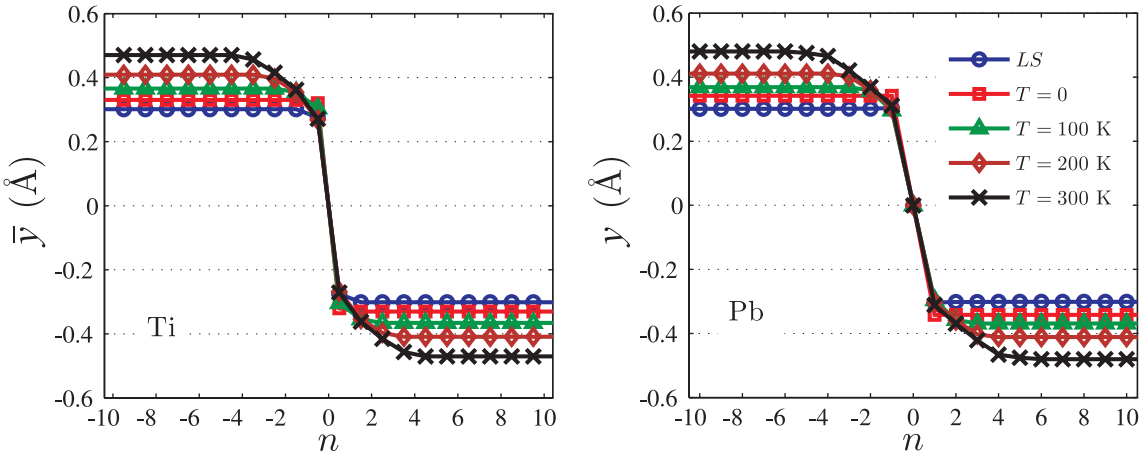

Fig. 2: (Colour on-line) The y-coordinates of Pb and Ti cores in the Pb-centered 180° domain wall as a function of temperature. LS denotes the lattice statics solution.

where $\mathcal{E}$ is the total static energy of the lattice and $\omega(\mathbf{k})$ is the frequency at wave number $\mathbf{k} \in \mathtt{B}$ with $\mathtt{B}$ the first Brillouin zone of the sublattices. Note that for calculating the derivatives of the frequencies, we exploit the analytical method of Kantorovich [15].

For optimization of the free energy, we use the quasi-Newton method with the Broyden-Fletcher-Goldfurb-Shanno update for calculating the approximate inverse Hessian in each step [23]. We should mention that to converge to the optimized configuration, one should select an initial configuration close to the solution. Thus, for calculating a finite-temperature configuration, we start with a nominal configuration (see fig. 1), which is obtained by relaxing the bulk at temperature $T = 0\,\mathrm{K}$, and then using this bulk configuration with opposite directions of core-shell shifts on the two sides of the 180° domain wall. Then, we relax the nominal configuration and obtain the lattice statics solution. Next, using the lattice statics solution, we obtain the lattice configuration at zero temperature and then we use temperature steps of $\Delta T = 25\,\mathrm{K}$, and obtain the optimized configuration at a given finite temperature. This way we observe that the quasi-Newton method converges relatively fast. Assuming a force tolerance of $0.05\,\mathrm{eV/\AA}$, our solutions converged after about 20 to 40 iterations depending on the temperature. Note that we only assume periodicity of unit cells in the y- and z-directions. In the x-direction we assume N unit cells in each side of the domain wall and use the temperature-dependent bulk configurations as the far-field boundary conditions. Our numerical experiments show that $N = 12$ would be enough to capture the atomic structure near the domain walls up to $T = 300\,\mathrm{K}$ as we do not see changes in the structure by choosing larger N. In our calculations, we used a $1 \times 3 \times 3$ k-point Monkhorst-Pack mesh [24]. Also for calculating the classical Coulombic potential and force, we used the damped Wolf method [25].

Numerical results for 180° domain walls. – Because displacements of core and shell of the same atom are close, we only report the core displacements. Figure 2 shows the y-coordinates (tetragonal coordinates) of the Pb and Ti cores relative to a Pb core on the Pb-centered domain wall. Figure 3 shows the y-coordinates of the Pb and Ti cores relative to a Ti core on the Ti-centered domain wall. In these figures $\bar{y} = y - (c/2)$, where c is the temperature-dependent lattice parameter in the tetragonal direction. The lattice parameters change with temperature such that by increasing temperature, unit cells transform from tetragonal to cubic [26]. Here to calculate lattice parameters at a finite temperature, we separately optimized the bulk lattice at that temperature. Note that far from the domain wall, each half-lattice approaches its corresponding temperature-dependent bulk configuration.

In these figures, LS denotes the lattice statics solution (static energy minimization). We observe that the lattice statics solution and the configuration obtained by the free-energy minimization at zero temperature although predicting nearly the same domain wall thicknesses, are different due to the zero-point motions; the lattice statics method ignores the quantum effects. It is known that zero-point motions can have significant effects in some systems [27]. Here we observe that zero-point motions affect the Ti-centered domain wall more than the Pb-centered domain wall; zero-point motions change the lattice statics solutions by about 15% in the Pb-centered domain wall and by about 50% in the Ti-centered domain wall. Since the atomic displacements normal to the domain wall are small (they are of order 10^{-2} Å) we do not report them here. However, we will comment on them in the sequel.

Increasing the temperature from 0 to 300 K, we observe that the domain wall thickness increases from 1 nm to about 3 nm. This qualitatively agrees with experimental

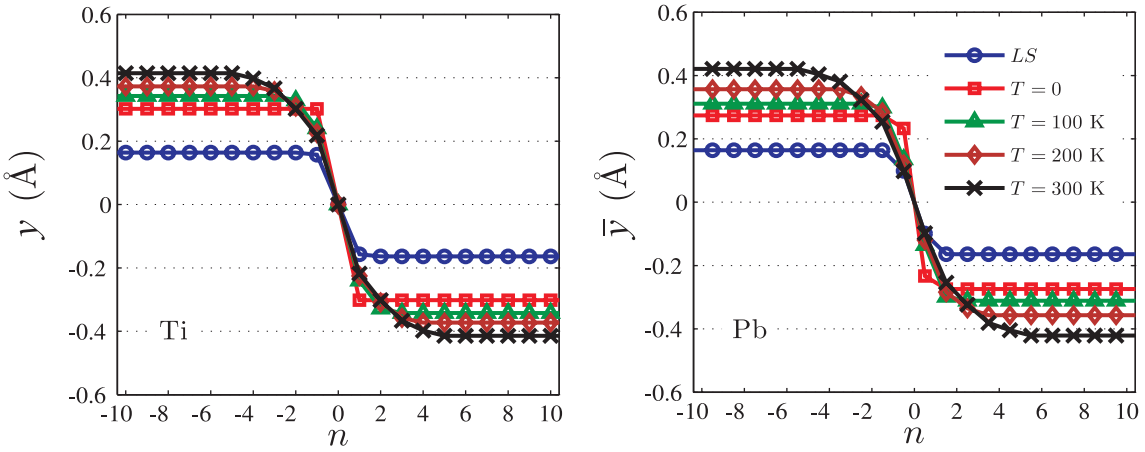

Fig. 3: (Colour on-line) The y-coordinates of Pb and Ti cores in the Ti-centered 180° domain wall as a function of temperature. LS denotes the lattice statics solution.

observations for 90° domain walls in $PbTiO_3$ by Foeth *et al.* [28] and domain walls in $LaAlO_3$ by Chrosch and Salje [8] who observed that domain wall thickness increases with temperature. They measured an average domain wall thickness from room temperature up to the Curie temperature. It is worth mentioning that from Ginzburg-Landau-Devonshire theory, domain wall thickness is proportional to $|T - T_c|^{-1}$ [8], where T_c is the Curie temperature. This means that for low temperatures domain wall thickness is linear in temperature. We observe this linear behavior in our numerical simulations. We should also mention that a similar trend was observed in a lattice of dipoles [21].

Note also that domain wall thickness cannot be defined uniquely very much like boundary layer thickness in fluid mechanics. Here, domain wall thickness is by definition the region that is affected by the domain wall, *i.e.* those layers of atoms that are distorted. One can use definitions like the 99%-thickness in fluid mechanics and define the domain wall thickness as the length of the region that has 99% of the far-field rigid translation displacement. What is important is that no matter what definition is chosen, domain wall "thickness" increases by increasing temperature.

Recently, it has been observed that there may be local normal and transverse polarizations near domain walls. For example, Goncalves-Ferreira *et al.* [29] observed local polarizations near domain wall of $CaTiO_3$ (nonpolar material) parallel and perpendicular to the wall plane. In our simulations, for both Pb- and Ti-centered domain walls we observe that polarization in c-direction switches within a few lattice spacings in the vicinity of the domain wall and the polarization normal to the domain wall is about 2% of the polarization in the c-direction. In particular, we see that normal displacements are 5.0% and 8.0% of their corresponding c-displacements in the Pb- and Ti-centered domain walls, respectively. This agrees with the results of Lee *et al.* [30] who observed non-zero displacements normal to the domain wall. In their calculations, polarization normal to the domain wall in

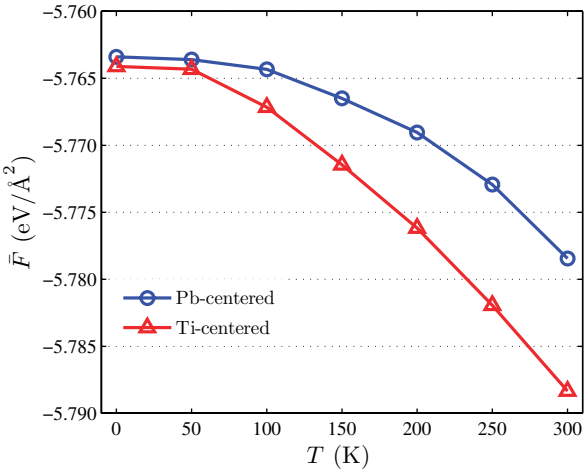

Fig. 4: (Colour on-line) Free energy of the domain walls as a function of temperature.

the Pb and Ti-centered 180° domain walls are 2.5% and 1.75%, respectively, of the bulk polarization.

In fig. 4, we have plotted the free energy per unit cell, $\bar{F} = F/(N \times a \times c)$, where N is the number of relaxed unit cells and a and c are temperature-dependent lattice parameters, for the two types of domain walls. In agreement with Meyer and Vanderbilt [3], we observe that Ti-centered domain walls have a higher static energy, however we see that they have a lower free energy and hence are the preferred domain wall configuration at finite temperatures.

Concluding remarks. – In this work we obtained the finite-temperature structure of Pb- and Ti-centered 180° domain walls in $PbTiO_3$ using a quasi-harmonic–lattice dynamics method. Our numerical results are in good agreement with experimental measurements. We observed a strong dependence of structure on temperature. In particular, 180° domain walls at $T = 300\,\mathrm{K}$ are three times thicker than those at $T = 0\,\mathrm{K}$. We also observed that

free energy is a decreasing function of temperature and free energy of a Ti-centered domain wall is always lower than that of a Pb-centered domain wall and hence Ti-centered domain walls are more likely to be seen at finite temperatures.

* * *

We thank an anonymous referee for useful comments.

REFERENCES

[1] Bhattacharya K. and Ravichandran G., *Acta Mater.*, **51** (2003) 5941.
[2] Dawber M., Rabe K. M. and Scott J. F., *Rev. Mod. Phys.*, **77** (2005) 1083.
[3] Meyer B. and Vanderbilt D., *Phys. Rev. B*, **65** (2001) 1.
[4] Padilla J., Zhong W. and Vanderbilt D., *Phys. Rev. B*, **53** (1996) R5969.
[5] Pöykkö S. and Chadi D. J., *Appl. Phys. Lett.*, **75** (1999) 2830.
[6] Yavari A., Ortiz M. and Bhattacharya K., *Philos. Mag.*, **87** (2007) 3997.
[7] Hlinka J. and Marton P., *Phys. Rev. B*, **74** (2006) 104104.
[8] Chrosch J. and Salje E. K. H., *J. Appl. Phys.*, **85** (1999) 722.
[9] Iwata M., Katsuraya K., Suzuki I., Maeda M., Yasuda N. and Ishibashi Y., *Jpn. J. Appl. Phys.*, **42** (2003) 6201.
[10] Lehnen P., Dec J. and Kleemann W., *J. Phys. D: Appl. Phys.*, **33** (2000) 1932.
[11] Shilo D., Ravichandran G. and Bhattacharya K., *Nat. Mater.*, **3** (2004) 453.
[12] Lee W. T., Salje E. K. H. and Bismayer U., *Phys. Rev. B*, **72** (2005) 104116.
[13] Angoshtari A. and Yavari A., *Comput. Mater. Sci.*, **48** (2010) 258.
[14] Asthagiri A., Wu Z., Choudhury N. and Cohen R. E., *Ferroelectrics*, **333** (2006) 69.
[15] Kantorovich L. N., *Phys. Rev. B*, **51** (1995) 3520.
[16] Kantorovich L. N., *Phys. Rev. B*, **51** (1995) 3535.
[17] Gale J. D., *J. Phys. Chem. B*, **102** (1998) 5423.
[18] Taylor M. B., Barrera G. D., Allan N. L. and Barron T. H. K., *Phys. Rev. B*, **56** (1997) 14380.
[19] Yavari A., Ortiz M. and Bhattacharya K., *J. Elast.*, **86** (2007) 41.
[20] Kavianpour S. and Yavari A., *Comput. Mater. Sci.*, **44** (2009) 1296.
[21] Yavari A. and Angoshtari A., *Int. J. Solids Struct.*, **47** (2010) 1807.
[22] Lesar R., Najafabadi R. and Srolovitz D. J., *Phys. Rev. Lett.*, **63** (1989) 624.
[23] Press W. H., Teukolsky S. A., Vetterling W. T. and Flannery B. P., *Numerical Recipes: The Art of Scientific Computing* (Cambridge University Press, Cambridge) 1989.
[24] Monkhorst H. J. and Pack J. D., *Phys. Rev. B*, **13** (1976) 5188.
[25] Wolf D. P., Keblinski P., Phillpot S. R. and Eggebrecht J., *J. Chem. Phys.*, **110** (1999) 8254.
[26] Behera R. K., Hinojosa B. B., Sinnott S. B., Asthagiri A. and Phillpot S. R., *J. Phys.: Condens. Matter*, **20** (2008) 395004.
[27] Kohanoff J., Andreoni W. and Parrinello M., *Phys. Rev. B*, **46** (1992) 4371.
[28] Foeth M., Stadelmann P. and Robert M., *Physica A*, **373** (2007) 439.
[29] Goncalves-Ferreira L., Redfern S. A. T., Artacho E. and Salje E. K. H., *Phys. Rev. Lett.*, **101** (2008) 097602.
[30] Lee D., Behera R. K., Wu P., Xu H., Li Y. L., Sinnott S. B., Phillpot S. R., Chen L. Q. and Gopalan V., *Phys. Rev. B*, **80** (2009) 060102(R).